ICASSP 2025 - 2025 IEEE International Conference on Acoustics, Speech and Signal Processing (ICASSP) | 979-8-3503-6874-1/25/$31.00 ©2025 IEEE | DOI: 10.1109/ICASSP49660.2025.10889435

Near-field AoA estimation with Complex Convolutional Kolmogorov-Arnold Network

Jiayi Wang
School of Electronic Information and Electrical Engineering
Shanghai Jiao Tong University
Shanghai, China
wangjiayi02@sjtu.edu.cn

Disheng Xiao
School of Electronic Information and Electrical Engineering
Shanghai Jiao Tong University
Shanghai, China
xiaodisheng@sjtu.edu.cn

Yingkai Cao
School of Electronic Information and Electrical Engineering
Shanghai Jiao Tong University
Shanghai, China
cyk923@sjtu.edu.cn

Kai Ying*
School of Electronic Information and Electrical Engineering
Shanghai Jiao Tong University
Shanghai, China
yingkai0301@sjtu.edu.cn

Ming Xiao
Division of Information Science and Engineering
KTH Royal Institute of Technology
Stockholm, Sweden
mingx@kth.se

***Abstract*—The development of 5G and beyond puts forward higher requirements for indoor positioning. However, conventional angle of arrival (AoA) estimation algorithms still rely on the far-field assumption, which is not applicable and may lead to a loss of accuracy. In this paper, we investigate the near-field AoA estimation problem and propose the complex convolutional Kolmogorov-Arnold network (CCKAN). With complex convolution, our method enhances the intrinsic relationship of signal amplitude and phase by simulating complex-valued operation in the convolution. We also introduce Kolmogorov-Arnold network (KAN), a deep learning model with better interpretability, as a feature extraction block. Results show that CCKAN achieves higher accuracy than other baseline methods in the near-field AoA estimation task. Furthermore, the model also exhibits remarkable reliability in both near-field and far-field cases.**

***Index Terms*—near-field, AoA estimation, complex convolution, KAN**

I. Introduction

The next generation of communication technology brings higher communication rate and capacity, and also enhances the sensing ability of communication systems [1]. Near-field sensing is an important research topic for indoor integrated sensing and communication (ISAC) [2], in which angle of arrival (AoA) estimation can provide spatial information for users [3].

Conventional algorithms for AoA estimation include Capon algorithm [4] and multiple signal classification (MUSIC) algorithm [5]. Based on linear constrained minimum variance (LCMV), Capon algorithm estimates the arrival angle by searching the peak value of the spatial spectrum function related to the steering vector. The MUSIC algorithm uses the orthogonality of signal subspace and noise subspace to construct spectrum function, which has higher AoA resolution than Capon. Both the Capon algorithm and MUSIC algorithm can be applied to near-field AoA estimation by expanding the search space and conducting joint estimation of angle and distance. However, due to the instability of statistical characteristics, conventional algorithms exhibit significant estimation errors when dealing with low snapshots and closely spaced sources.

Recently, the data-driven AoA estimation method has achieved great success. Authors in [6] introduced convolutional neural networks (CNNs) to predict AoA using sample convariance matrix estimation. Authors in [7] proposed the DeepMUSIC architecture, which divides the estimation results into several sub-regions and utilizes multiple independent CNNs to learn the mapping relationships corresponding to these sub-regions. The above mentioned researches achieve lower complexity and better robustness than conventional algorithms, but they do not take the near-field effect into consideration. Authors in [8] proposed a grid-based high-resolution deep learning source localization (DLSL) algorithm to adapt to the near-field situation. By classifying multiple source location categories, the near-field AoA estimation performances and ranges are comprehensively improved. However, the intrinsic correlation between real and imaginary parts in complex-valued signals is overlooked, which may lead to the loss of phase information contained in original signals, and thus subsequently cause a decrease in estimation accuracy.

In order to solve the problem of near-field AoA estimation, we propose complex convolutional Kolmogorov-Arnold network (CCKAN) in this paper. This model introduces complex convolutional networks into Kolmogorov-Arnold network (KAN), which can make full use of complex-valued signals as input and avoid information loss caused by dividing signals into irrelevant real and imaginary parts. At the same time, the hierarchical feature construction ability of KAN decomposes the output data of complex convolutional networks into multiple simple features. Thereby, KAN can better fit AoA with higher accuracy. Results demonstrate that our algorithm

achieves an excellent AoA resolution in both far-field and near-field conditions.

II. System Model

A. Near-Field Propagation Model

We consider an indoor multiple input multiple output (MIMO) near-field communication scenario consisting of N uniform linear antenna access points (APs) at $\frac{\lambda}{2}$ intervals, where λ denotes wavelength. According to the assumptions of the conventional algorithm, the signal reaches the receiving antenna in the form of plane waves. However, denote the array aperture by D, when the communication distance r of the user device meets $0.62(\frac{D^3}{\lambda})^{\frac{1}{2}} < r < \frac{2D^2}{\lambda}$, device is located in the near-field region (Fresnel region) of the array [9]. In this case, the above assumption fails and the signal will reach the receiving antenna in the form of spherical wave propagation. Assume that $D = 1$ m, the carrier frequency $f = 12$ GHz, and the Rayleigh distance [9] is up to 80 m, which is significantly longer than the average indoor scene. In this scenario, the effect of near-field signals is of great significance.

We first formulate the analysis of the received signal affected by the near-field effect. It is assumed that the central antenna of N uniform linear antennas is the n_c-th antenna, which is set as a reference point. There are M user devices communicating with the receiving array in the near-field region. The distance between the m-th user devices and the reference point is r_m [10]. At each time instance $t \in \{1, \ldots, T\}$, the received signal $\boldsymbol{x}(t) = [x_1(t), \ldots, x_N(t)] \in \mathbb{C}^N$ acquired by the receiver is written as:

$$\boldsymbol{x}(t) = \mathbf{A}(\boldsymbol{\theta}, \boldsymbol{r})\boldsymbol{s}(t) + \boldsymbol{\omega}(t), \tag{1}$$

where $\boldsymbol{s}(t) = [s_1(t), \ldots, s_M(t)] \in \mathbb{C}^M$ is the source signal vector from AoAs $\boldsymbol{\theta} = [\theta_1, \ldots, \theta_M] \in \mathbb{C}^M$, and distance $\boldsymbol{r} = [r_1, \ldots, r_m, \ldots, r_M] \in \mathbb{C}^M$. $\boldsymbol{\omega}(t) = [\omega_1(t), \ldots, \omega_n(t), \ldots, \omega_N(t)] \in \mathbb{C}^N, 1 \leq n \leq N$ is the noise vector, whose elements follow a zero-mean Gaussian distribution. $\mathbf{A}(\boldsymbol{\theta}, \boldsymbol{r}) = [\boldsymbol{a}_1(\theta_1, r_1), \ldots, \boldsymbol{a}_M(\theta_M, r_M)]$ denotes steering vectors. In the following, we will abbreviate $\mathbf{A}(\boldsymbol{\theta}, \boldsymbol{r})$ as $\mathbf{A}$.

The AoA for the m-th target source to the receiver is θ_m, $\theta_m \in [-\frac{\pi}{2}, \frac{\pi}{2}]$, and the corresponding distance is r_m. Thereby, the array steering vector of the m-th source can be expressed as:

$$\boldsymbol{a}_m(\theta_m, r_m) = [a_{1,m}, \ldots, a_{n,m}, \ldots, a_{N,m}]^T, \tag{2}$$

where

$$a_{n,m} = \kappa_{n,m} \exp\left[-j\frac{2\pi}{\lambda}\left(r_{n,m} - r_m\right)\right]. \tag{3}$$

In (3), $r_{n,m}$ is the distance from the n-th antenna to the m-th target source. $\kappa_{n,m} = \frac{r_m}{r_{n,m}}$ is the relative amplitude, and according to the law of cosine, we have

$$r_{n,m} = \sqrt{r_m^2 + \delta_n^2 d^2 - 2r_m \delta_n d \sin\theta_m}, \tag{4}$$

where $\delta_n = n - n_c$.

B. 2D-MUSIC Algorithm

For the far-field model, MUSIC algorithm uses the orthogonality of signal subspace and noise subspace to construct spatial spectrum function. Then it estimates the AoAs through spectral peak search. In the case of near-field, the MUSIC algorithm is still applicable, and it conducts a two-dimensional (2D) search to jointly estimate the arrival angle and distance, which is also called 2D-MUSIC algorithm [11].

Assuming that the sampling time is greater than the coherence time. The received signal covariance matrix $\hat{\mathbf{R}} \in \mathbb{C}^{N \times N}$ obtained from finite sampling is shown as:

$$\begin{aligned}\hat{\mathbf{R}} &= \mathbb{E}\left[\boldsymbol{x}(t)\,\boldsymbol{x}^{\mathrm{H}}(t)\right] \\ &= \mathbf{A}\mathbb{E}\left[\boldsymbol{s}(t)\,\boldsymbol{s}^{\mathrm{H}}(t)\right]\mathbf{A}^{\mathrm{H}} + \mathbb{E}\left[\boldsymbol{\omega}(t)\,\boldsymbol{\omega}^{\mathrm{H}}(t)\right] \\ &= \boldsymbol{\Xi}_{\mathrm{S}}\boldsymbol{\Lambda}_{\mathrm{S}}\boldsymbol{\Xi}_{\mathrm{S}}^{\mathrm{H}} + \boldsymbol{\Xi}_{\mathrm{W}}\boldsymbol{\Lambda}_{\mathrm{W}}\boldsymbol{\Xi}_{\mathrm{W}}^{\mathrm{H}},\end{aligned} \tag{5}$$

where $(\cdot)^{\mathrm{H}}$ denotes Hermitian transpose, $\mathbb{E}[\cdot]$ means the expectation, $\boldsymbol{\Xi}_{\mathrm{S}}$ is a signal subspace composed of eigenvectors corresponding to large eigenvalues, $\boldsymbol{\Xi}_{\mathrm{W}}$ is a noise subspace composed of eigenvectors corresponding to small eigenvalues, $\boldsymbol{\Lambda}_{\mathrm{S}}$ and $\boldsymbol{\Lambda}_{\mathrm{W}}$ represent the eigenvalue matrix of signal subspace and noise subspace respectively.

By conducting a 2D search for r and θ, the spatial spectrum is

$$\mathrm{P}(\theta, r) = \frac{1}{\boldsymbol{a}^{\mathrm{H}}(\theta, r)\,\boldsymbol{\Xi}_{\mathrm{W}}\boldsymbol{\Xi}_{\mathrm{W}}^{\mathrm{H}}\boldsymbol{a}(\theta, r)}. \tag{6}$$

The estimation results of 2D-MUSIC algorithm $\hat{\boldsymbol{\theta}} = [\hat{\theta}_1, \ldots, \hat{\theta}_M]$ and $\hat{\boldsymbol{r}} = [\hat{r}_1, \ldots, \hat{r}_M]$ can be determined by looking for M main peaks of the spatial spectrum.

As a conventional method for near-field AoA estimation, 2D-MUSIC algorithm has an intrinsic limitation that it cannot accurately estimate AoAs with a small number of snapshots, because $\hat{\mathbf{R}}$ needs enough observation data to average the statistical properties of noise and signal. Furthermore, the peak spectrum can not be distinguished for close signals due to overlapping, resulting in a decrease of accuracy.

III. Deep Learning Model

In the AoA estimation problem, models need to deal with complex-valued signals that contain both amplitude and phase information. However, conventional data-driven methods often ignore the correlation between amplitude and phase. Besides, the low interpretability of the conventional network structures is a tough challenge. Inspired by [12] and [13], we designed CCKAN to overcome these limitations and apply it in the AoA estimation task. This model is shown in Fig. 1.

A. Complex Convolutional Networks

The complex convolutional networks proposed in this paper can perform convolution, normalization and activation of complex input. The essence of this method is to simulate complex-valued operation in the internal mechanism [12]. In the l-th

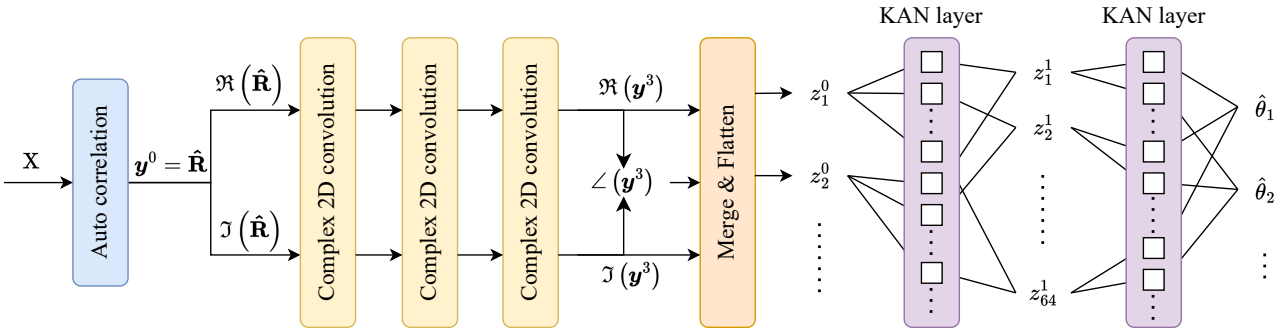

Fig. 1. CCKAN model, each complex 2D convolution block also includes complex batch normalization and $\mathbb{C}$ReLU layers

layer network, the input, weight matrix and bias vector are expressed as:

$$\begin{aligned} \boldsymbol{y}^l &= \boldsymbol{u}^l + j\boldsymbol{v}^l, \\ \mathbf{W}^l &= \mathbf{W}_{\mathrm{R}}^l + j\mathbf{W}_{\mathrm{I}}^l, \\ \mathbf{b}^l &= \mathbf{b}_{\mathrm{R}}^l + j\mathbf{b}_{\mathrm{I}}^l, \end{aligned} \tag{7}$$

where $\boldsymbol{u}^l, \mathbf{W}_{\mathrm{R}}^l, \mathbf{b}_{\mathrm{R}}^l$ respectively correspond to the real parts of $\boldsymbol{y}^l, \mathbf{W}^l, \mathbf{b}^l$; and $\boldsymbol{v}^l, \mathbf{W}_{\mathrm{I}}^l, \mathbf{b}_{\mathrm{I}}^l$ respectively correspond to the imaginary parts of $\boldsymbol{y}^l, \mathbf{W}^l, \mathbf{b}^l$.

Complex Convolution In order to perform 2D convolution equivalent in the complex domain, we use real-valued entities to simulate complex operations, which are expressed as:

$$\begin{bmatrix} \Re\left(\mathbf{W}^l * \boldsymbol{y}^l\right) \\ \Im\left(\mathbf{W}^l * \boldsymbol{y}^l\right) \end{bmatrix} = \begin{bmatrix} \mathbf{W}_{\mathrm{R}}^l & -\mathbf{W}_{\mathrm{I}}^l \\ \mathbf{W}_{\mathrm{I}}^l & \mathbf{W}_{\mathrm{R}}^l \end{bmatrix} * \begin{bmatrix} \boldsymbol{u}^l \\ \boldsymbol{v}^l \end{bmatrix}, \tag{8}$$

where $*$ is the convolution operation.

Complex Batch Normalization As the same as conventional batch normalization methods which begin with a standard normal distribution of inputs, complex inputs also require a standard complex distribution, which can be achieved by

$$\widetilde{\boldsymbol{y}}^l = \mathbf{V}^{-\frac{1}{2}}\left(\boldsymbol{y}^l - \mathbb{E}\left[\boldsymbol{y}^l\right]\right), \tag{9}$$

where

$$\mathbf{V} = \begin{pmatrix} \mathrm{Cov}\left(\Re\left(\boldsymbol{y}^l\right), \Re\left(\boldsymbol{y}^l\right)\right) & \mathrm{Cov}\left(\Re\left(\boldsymbol{y}^l\right), \Im\left(\boldsymbol{y}^l\right)\right) \\ \mathrm{Cov}\left(\Im\left(\boldsymbol{y}^l\right), \Re\left(\boldsymbol{y}^l\right)\right) & \mathrm{Cov}\left(\Im\left(\boldsymbol{y}^l\right), \Im\left(\boldsymbol{y}^l\right)\right) \end{pmatrix}. \tag{10}$$

Finally, complex batch normalization can be defined as:

$$\mathrm{BN}\left(\widetilde{\boldsymbol{y}}^l\right) = \boldsymbol{\gamma}\widetilde{\boldsymbol{y}}^l + \boldsymbol{\beta}, \tag{11}$$

where $\boldsymbol{\gamma}$ is a 2×2 semi-definite matrix composed of three learnable components, and $\boldsymbol{\beta}$ is a complex translation parameter composed of two learnable components.

$\mathbb{C}$ReLU We apply $\mathbb{C}$ReLU proposed in [12] as the activation function, which applies ReLU to the real and imaginary parts of the input vector, i.e:

$$\mathbb{C}\mathrm{ReLU}\left(y^l\right) = \mathrm{ReLU}\left(u^l\right) + j\mathrm{ReLU}\left(v^l\right). \tag{12}$$

In order to construct the input data of KAN, we stack the real part, imaginary part and angle value of the output of complex convolutional networks to get the real-valued data.

B. Kolmogorov-Arnold Network

KAN is designed to efficiently learn and approximate complex high-dimensional functions by decomposing them into a series of simpler functions [13]. Suppose the shape of KAN is $[n_0, \ldots, n_L]$. Between l-th layer and $(l+1)$-th layer, there are $n_l n_{l+1}$ activation functions, defined as $\phi_{l,i,j}$, $l = 0, \ldots, L-1$, $i = 1, \ldots, n_{l+1}$, $j = 1, \ldots, n_l$. Each KAN layer can be represented as a matrix

$$\boldsymbol{z}^{l+1} = \begin{pmatrix} \phi_{l,1,1}(\cdot) & \cdots & \phi_{l,1,n_l}(\cdot) \\ \cdots & \ddots & \cdots \\ \phi_{l,n_{l+1},1}(\cdot) & \cdots & \phi_{l,n_{l+1},n_l}(\cdot) \end{pmatrix} \boldsymbol{z}^l. \tag{13}$$

The hierarchical structure of KAN facilitates the model's ability to map the real-valued angle from the complex-valued output. KAN extracts AoA related features at different scales and levels of abstraction, thus describing AoA comprehensively and accurately.

C. Training Procedure

We treat the near-field AoA estimation as a multiple regression problem. CCKAN is trained in a supervised manner. For evaluation, the output $\hat{\boldsymbol{\theta}} = [\hat{\theta}_1, \ldots, \hat{\theta}_M]$ is compared with ground truth $\boldsymbol{\theta}$ using the root mean square period error (RMSPE) [14]:

$$\mathrm{RMSEP}\left(\boldsymbol{\theta}, \hat{\boldsymbol{\theta}}\right) = \min_{\mathbf{P} \in \mathcal{P}_M} \left(\frac{1}{M}\left\|\mathrm{mod}_\pi\left(\boldsymbol{\theta} - \mathbf{P}\hat{\boldsymbol{\theta}}\right)\right\|^2\right)^{\frac{1}{2}}, \tag{14}$$

where $\mathcal{P}_M$ is the set of all permutations of $M \times M$.

IV. Empirical Study

A. Experimental Setup

The system considered in our experiment is an indoor MIMO communication scenario within Rayleigh distance. The specific system parameters are shown in Table I. For the distance parameter $\boldsymbol{r}$, we select it uniformly in Fresnel region. All datasets utilized in our experiments were generated through numerical simulations. For each experimental scenario, we collected 10000 frames of received signals, with each frame containing 200 snapshots. These signal frames were divided into non-overlapping training and testing sets with a ratio of 8:2. The remaining parameters and dataset configurations were maintained identical to those reported in [15].

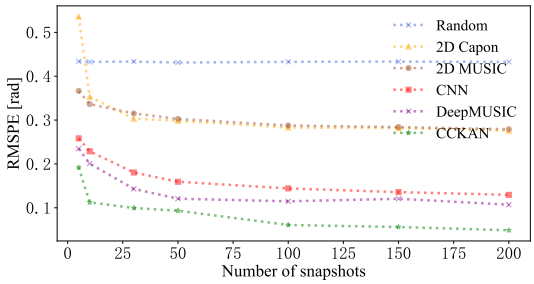

Fig. 2. Change the number of snapshots in the near-field

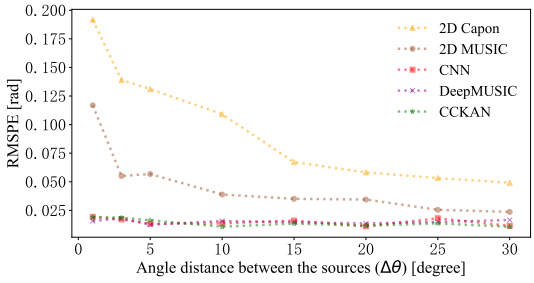

Fig. 3. Near-field AoA estimation of $M = 2$ closely spaced sources

The proposed algorithm shown in Fig. 1 is implemented as follows. The input $\mathbf{X}$ is stacked from $\boldsymbol{x}(t)$ sampled by $T = 200$ time instances, and then transformed into $\hat{\mathbf{R}}$ using empirical auto correlation. Then $\hat{\mathbf{R}}$ is divided into real part $\Re(\hat{\mathbf{R}})$ and imaginary part $\Im(\hat{\mathbf{R}})$. They serve as the input $\boldsymbol{y}^0$ of the complex convolutional network. The network uses four complex 2D convolution, and after each convolution, complex batch normalization and $\mathbb{C}$ReLU are used for processing. Next, the output data $\Re(\boldsymbol{y}^3)$, $\Im(\boldsymbol{y}^3)$ and $\angle(\boldsymbol{y}^3)$ are merged and flattened, serving as the input of the two-layer KAN, whose middle output dimension is 64. For each KAN layer, the number of grid intervals is 5, and the order of piecewise polynomial is 3. The final output is mapped to $[-\frac{\pi}{2}, \frac{\pi}{2}]$.

We take Capon algorithm [4] and MUSIC algorithm [5] as representative algorithms among classical algorithms. For near-field experiments, these methods are extended to 2D Capon and 2D MUSIC to accommodate. Besides, we use CNN [6] and DeepMUSIC [7] models as baselines among deep learning models to verify the effectiveness of CCKAN. Random represents that the estimated angle is randomly selected. The performance evaluation was conducted using RMSPE metric, and the results were averaged across 100 independent Monte Carlo simulations.

TABLE I
SIMULATION PARAMETERS

Parameter	Value	Parameter	Value
Array elements N	8	SNR	10 dB
Array length D	0.105 m	Optimizer	Adam [16]
Wave length λ	0.03 m	Learning rate	0.01
Snapshot T	200	Data size L	1×10^4

B. Results

Fig. 2 shows the relationship between estimation accuracy and the number of snapshots when $M = 5$. The results demonstrate that CCKAN is always better than other neural network models. As for the conventional algorithms, they crash when the number of snapshots is below 10.

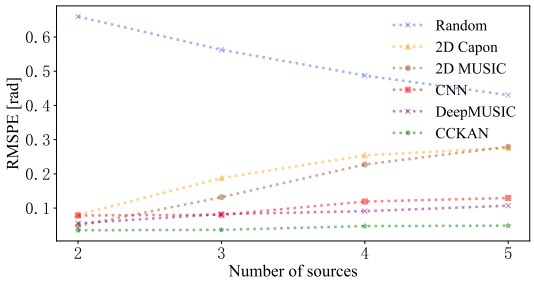

Fig. 4. Change the number of sources in the near-field

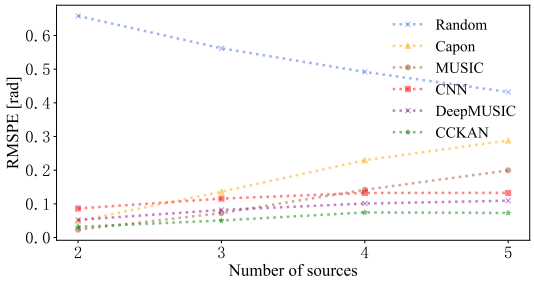

Fig. 5. Change the number of sources in the far-field

In order to compare the resolution of these algorithms for close spaced source signals, we calculate the RMSPE of two signal sources at different angle distance. As shown in Fig. 3, CCKAN has the lowest rate of errors and the deep learning algorithm shows a constant low error in all cases. However, for the conventional algorithms, they decrease significantly at $\Delta\theta = 5$. This indicates that the deep learning algorithm has a higher resolution in angle estimation than the conventional algorithms.

Under near-field conditions and far-field conditions, the relationship between the estimation accuracy and the number of sources is shown in Fig. 4 and Fig. 5. The results indicate that the conventional algorithms are greatly affected by the number of sources, and the accuracy of conventional algorithms decreases rapidly when the number of sources increases. Generally, the algorithm of deep learning has better accuracy for situations with a large number of sources, and CCKAN can achieve optimal accuracy in most scenarios. Comparing Fig. 4 and Fig. 5, we can see that the conventional AoA estimation algorithm degenerates more in near-field conditions compared with far-field conditions. This result shows that CCKAN algorithm has better robustness in such case.

V. CONCLUSIONS

In this paper, we study the AoA estimation problem for near-field signals and propose CCKAN. The proposed complex convolutional networks can directly deal with complex-valued features, which reduces the loss of amplitude and phase information caused by conventional neural network models. And KAN is introduced to improve the interpretability of the model. Results demonstrate that the near-field AoA estimation performance of CCKAN is obviously better than other baseline methods. In addition, it can maintain satisfactory results even when extended to other snapshot numbers and far-field conditions.

REFERENCES

[1] Yongsen Ma, Gang Zhou, and Shuangquan Wang, "WiFi sensing with channel state information: A survey," *ACM Computing Surveys (CSUR)*, vol. 52, no. 3, pp. 1–36, 2019.

[2] Zhaolin Wang, Xidong Mu, and Yuanwei Liu, "Near-field integrated sensing and communications," *IEEE Communications Letters*, vol. 27, no. 8, pp. 2048–2052, 2023.

[3] Grega Morano, Aleš Simončič, Teodora Kocevska, Tomaž Javornik, and Andrej Hrovat, "Angle of arrival estimation using IEEE 802.15.4 TSCH protocol," in *2023 IEEE 34th Annual International Symposium on Personal, Indoor and Mobile Radio Communications (PIMRC)*. IEEE, 2023, pp. 1–7.

[4] Jack Capon, "High-resolution frequency-wavenumber spectrum analysis," *Proceedings of the IEEE*, vol. 57, no. 8, pp. 1408–1418, 1969.

[5] Ralph Schmidt, "Multiple emitter location and signal parameter estimation," *IEEE transactions on antennas and propagation*, vol. 34, no. 3, pp. 276–280, 1986.

[6] Georgios K Papageorgiou, Mathini Sellathurai, and Yonina C Eldar, "Deep networks for direction-of-arrival estimation in low SNR," *IEEE Transactions on Signal Processing*, vol. 69, pp. 3714–3729, 2021.

[7] Ahmet M Elbir, "DeepMUSIC: Multiple signal classification via deep learning," *IEEE Sensors Letters*, vol. 4, no. 4, pp. 1–4, 2020.

[8] Hojun Lee, Yongcheol Kim, Seunghwan Seol, and Jaehak Chung, "Deep learning-based near-field source localization without a priori knowledge of the number of sources," *IEEE Access*, vol. 10, pp. 55360–55368, 2022.

[9] John Sherman, "Properties of focused apertures in the fresnel region," *IRE Transactions on Antennas and Propagation*, vol. 10, no. 4, pp. 399–408, 1962.

[10] Yuanwei Liu, Zhaolin Wang, Jiaqi Xu, Chongjun Ouyang, Xidong Mu, and Robert Schober, "Near-field communications: A tutorial review," *IEEE Open Journal of the Communications Society*, 2023.

[11] Francesco Belfiori, Wim van Rossum, and Peter Hoogeboom, "Application of 2D MUSIC algorithm to range-azimuth FMCW radar data," in *2012 9th European Radar Conference*. IEEE, 2012, pp. 242–245.

[12] Chiheb Trabelsi, Olexa Bilaniuk, Ying Zhang, Dmitriy Serdyuk, Sandeep Subramanian, Joao Felipe Santos, Soroush Mehri, Negar Rostamzadeh, Yoshua Bengio, and Christopher J Pal, "Deep complex networks," *arXiv preprint arXiv:1705.09792*, 2017.

[13] Ziming Liu, Yixuan Wang, Sachin Vaidya, Fabian Ruehle, James Halverson, Marin Soljačić, Thomas Y Hou, and Max Tegmark, "KAN: kolmogorov-arnold networks," *arXiv preprint arXiv:2404.19756*, 2024.

[14] Tirza Routtenberg and Joseph Tabrikian, "Bayesian parameter estimation using periodic cost functions," *IEEE transactions on signal processing*, vol. 60, no. 3, pp. 1229–1240, 2011.

[15] Julian P Merkofer, Guy Revach, Nir Shlezinger, Tirza Routtenberg, and Ruud JG Van Sloun, "DA-MUSIC: Data-driven DoA estimation via deep augmented MUSIC algorithm," *IEEE Transactions on Vehicular Technology*, 2023.

[16] Diederik P. Kingma and Jimmy Ba, "Adam: A method for stochastic optimization," *CoRR*, vol. abs/1412.6980, 2014.